

Cascade embedding triethyltryptophanium iodide ionic liquid ($\text{TrpEt}_3^+ \text{I}^-$) on silicated titanomagnetite core ($\text{Fe}_{3-x}\text{Ti}_x\text{O}_4\text{-SiO}_2@ \text{TrpEt}_3^+ \text{I}^-$): A novel nano organic–inorganic hybrid to prepare a library of 4-substituted quinoline-2-carboxylates and 4,6-disubstituted quinoline-2-carboxylates

Kobra Nikoofar  | Fatemeh Molaei Yielzoleh

Department of Chemistry, Faculty of Physics and Chemistry, Alzahra University, Tehran, Iran

Correspondence

Kobra Nikoofar, Department of Chemistry, Faculty of Physics & Chemistry, Alzahra University, Tehran, Iran.

Email: k.nikoofar@alzahra.ac.ir; kobranikoofar@yahoo.com

Funding information

Alzahra University

Abstract

A library of substituted quinolone-2-carboxylates (4,6-disubstituted quinolone-2-carboxylates, 6-substituted quinoline dialkyl-2,4-dicarboxylates, and 6-substituted 4-[2-methoxy-2-oxoethyl]quinoline-2-methylcarboxylates) was obtained through different scopes of one-pot and one-step MCRs such as (a) three-component reaction of aromatic amines, dialkyl acetylenedicarboxylates, and terminal alkenes/ketones; (b) pseudo three-component reaction of anilines and dialkyl acetylenedicarboxylates; and (c) pseudo three-component reaction of anilines and methyl propiolate under solvent-free conditions at 100°C. The promoter of these annulation processes is a novel inorganic–organic core–shell that was obtained from silicated titanomagnetite, tryptophan amino acid, and ethyl iodide. The tryptophan embedded on the silicated titanomagnetite core ($\text{Fe}_{3-x}\text{Ti}_x\text{O}_4\text{-SiO}_2$) followed by alkylation with ethyl iodide subsequently result in situ preparation of triethyltryptophanium iodide ionic liquid ($\text{TrpEt}_3^+ \text{I}^-$). The final nanohybrid ($\text{Fe}_{3-x}\text{Ti}_x\text{O}_4\text{-SiO}_2@ \text{TrpEt}_3^+ \text{I}^-$) was characterized by field-emission scanning electron microscope, EDAX, FT-IR, TGA/DTG, vibrating sample magnetometer, and X-ray fluorescence techniques. The highlighted features of the protocol are as follows: (a) synthesis of a vast range of substituted quinolines through a straightforward method from simple substrates under solvent-free conditions, (b) utilizing various scopes of functionalities as substrates, (c) simple separation of the nano promoter via an external magnet, (d) regioselectivity in the cascade annulation procedure, and (e) recovery and reusability of the nanocomposite within three runs without significant activity loss.

KEYWORDS

2,4-disubstituted quinolines, annulation, ionic liquid, nano $\text{Fe}_{3-x}\text{Ti}_x\text{O}_4\text{-SiO}_2@ \text{TrpEt}_3^+ \text{I}^-$, titanomagnetite, tryptophan

1 | INTRODUCTION

Quinoline (benzo[b]pyridine or 1-azanaphthalene) is an applicant of *N*-containing heterocyclic motif in chemistry, medicine, and biology. Various kinds of compounds bearing quinolone building-blocks demonstrated numerous properties such as antitumor,^[1] anti-inflammatory,^[2] antiviral,^[3] antimalarial,^[4] antifungal,^[5] antibacterial,^[6] anticancer,^[7] antipsychotic,^[8] anti-HIV,^[9] antituberculosis,^[10] and antioxidant^[11] activities. In addition, various quinolone-containing compounds, applied in several branches of science and technology, exhibited interesting properties like electrochemical and antiplasmodium properties,^[12] fluorescence and cell imaging,^[13] optoelectronic,^[14] and rubber chemicals.^[15]

2,4-Substituted quinolines prepared via several methods such as cascade annulation of anilines with alkyne esters in a 1:2 M ratio in the presence of Cu(OTf)₂/HOTf,^[16] iron-catalyzed intermolecular [4 + 2] cyclization of aryl nitrones with geminal-substituted vinyl acetates,^[17] A₃-coupling between an aldehyde, amine, and alkyne,^[18] silver-catalyzed [3 + 1 + 2] annulation of simple amines, alkyne esters and terminal alkynes,^[19] DDQ-promoted three-component reaction of *o*-amino arylketones, aldehydes, and ammonium acetate,^[20] Cu(OAc)₂·H₂O catalyzed domino reaction of primary arylamines and terminal alkynes in a 1:2 M ratio,^[21] and multicomponent reaction of aniline, 2-nitro benzaldehyde, and propargyl alcohol in the presence of copper bromide.^[22]

Magnetic nanoparticles attracted special attention based on their unique properties and exploited in various scopes including multimodal photoacoustic, photothermal and photomechanical contrast agents,^[23] cancer nanotheranostic,^[24] antimicrobial drug delivery,^[25] electrochemical sensing,^[26] and magnetic resonance imaging.^[27]

Recently, the well-known magnetite (Fe₃O₄) is utilized in many catalytic fields such as wastewater treatment,^[28] Fenton-like degradation of tetracycline (as an organic pollutant),^[29] upgrading of heavy oil,^[30] and organic synthesis.^[31] The significance of nanomagnetite in the organic synthesis progressing area attributed to its easy production procedure, high functionalization capacity, large surface area, good stability, low toxicity and cost, simple isolation from the reaction media through an external magnet, and great recoverability and reusability without decreasing activity.

Titanomagnetite (Fe_{3-x}Ti_xO₄) is an interesting magnetized species, which is the objective in decolorization of methylene blue.^[32] In addition, many catalytic systems were prepared based on titanomagnetite to promote different kinds of organic transformations like synthesis of dihydropyrano[3,2-*c*]chromen-2-ones,^[33] tetrahydrobenzo

[*b*]pyrans, and dihydropyrano[2,3-*c*]pyrazoles synthesis,^[34] hexahydroquinolines,^[35,36] and 2,3-dihydroquinazolin-4 (*1H*)-ones.^[37]

Ionic liquids (ILs) are organic/inorganic salts with a melting point often below 100°C, low vapor pressure, low toxicity, high ion density and ionic conductivity, high chemical stabilities, and nonflammability. ILs possess wide-spread availability through changeable cations and anions that play dual crucial role in organic chemistry as exclusive catalyst/reaction media.^[38–40]

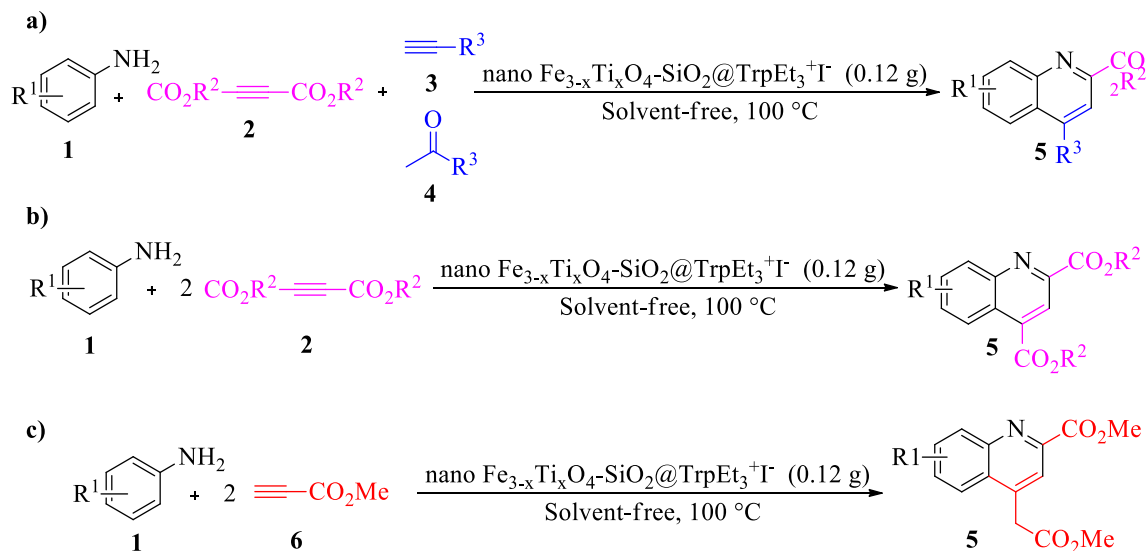
Amino acid ionic liquids (AAILs) were utilized recently in many aspects of scientific and technological fields as lubricants,^[41] metal Scavenging,^[42] ligand-exchange chiral separations,^[43] CO₂ absorbants,^[44] and self-assembly media of amphiphiles.^[45] The catalytic efficacy of some AAILs observed in the Morita–Baylis–Hillman reaction,^[46] Knoevenagel condensation,^[47] thiol-Michael addition,^[48] and Baeyer–Villiger oxidation of cyclic ketones.^[49]

In following our research preference to design novel nanostructures and investigation of their catalytic activity in heterocycles synthesis,^[50–54] herein, we report a novel multi-layered inorganic–organic hybrid gained from silicated titanomagnetite, tryptophan amino acid, and ethyl iodide (nano Fe_{3-x}Ti_xO₄-SiO₂@TrpEt₃⁺I⁻). In fact, the shell is an AAIL obtained in situ from tryptophan and ethyl iodide that anchored into the silica-titanomagnetized core step by step. The catalytic efficiency of the inorganic–bioorganic composite is examined in the solvent-free regioselective cascade annulations to prepare a library of substituted quinolones, which are as follows: (a) 4-, 6-disubstituted quinoline-2-carboxylates via the three-component reaction of aromatic amines, dialkyl acetylenedicarboxylates, and terminal alkenes/ketones; (b) 6-substituted quinoline dialkyl-2,4-dicarboxylates through the pseudo three-component reaction of anilines and dialkyl acetylenedicarboxylates; and (c) 6-substituted 4-(2-methoxy-2-oxoethyl)quinoline-2-methylcarboxylates by pseudo three-component reaction of anilines and methyl propiolate at 100°C (Scheme 1).

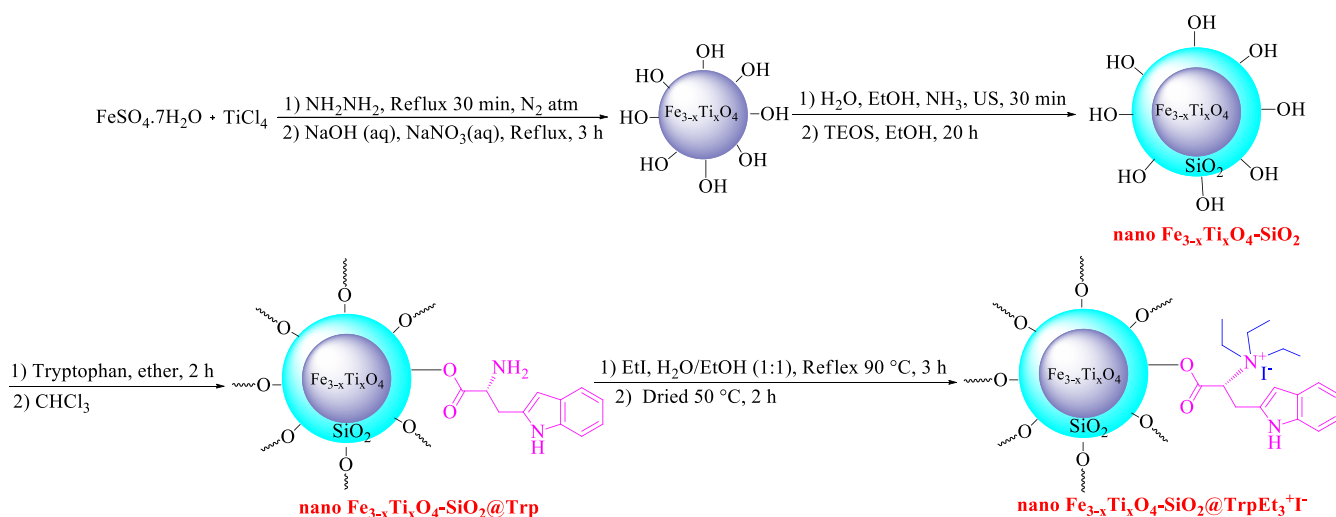
2 | RESULTS AND DISCUSSION

2.1 | Characterization of the nanocatalyst

The schematic preparing procedure of nano Fe_{3-x}Ti_xO₄-SiO₂@TrpEt₃⁺I⁻ is illustrated in Scheme 2. In the first step, titanomagnetite was prepared from titanium tetrachloride and ferrous sulfate heptahydrate, subsequent by the reaction with tetraethyl orthosilicate (TEOS) to obtain nano Fe_{3-x}Ti_xO₄-SiO₂. In order to seat the novel IL



SCHEME 1 Preparation of a library of substituted quinolines in the presence of nano $\text{Fe}_{3-x}\text{Ti}_x\text{O}_4\text{-SiO}_2\text{@TrpEt}_3^+\text{I}^-$



SCHEME 2 Schematic preparation procedure of nano $\text{Fe}_{3-x}\text{Ti}_x\text{O}_4\text{-SiO}_2\text{@TrpEt}_3^+\text{I}^-$

tertiethyl tryptophanium iodide ($\text{TrpEt}_3^+\text{I}^-$) on this core, a tandem two-step process was performed. Firstly, the amino acid tryptophan was embedded followed by adding ethyl iodide to yield the final silica coated titanomagnetite-IL nanocomposite (nano $\text{Fe}_{3-x}\text{Ti}_x\text{O}_4\text{-SiO}_2\text{@TrpEt}_3^+\text{I}^-$). The IL part is also obtained separately and characterized with physical and spectral data expressed in Section 3.3.

The FTIR spectra for successive preparation of the nanocomposite $\text{Fe}_{3-x}\text{Ti}_x\text{O}_4\text{-SiO}_2\text{@TrpEt}_3^+\text{I}^-$ are illustrated in Figure 1. According to Figure 1a, the bond at 588, 736, and $3,419\text{ cm}^{-1}$ attributed to symmetric stretching vibrations of Fe—O, Ti—O, and O—H bonds, respectively. In Figure 1b, appearance of the bands at

$1,214\text{ cm}^{-1}$ (stretching vibration of Si—O—Si group) affirmed the presence of silica layer on the titanomagnetite core. The stretching vibration of silanol of silica ($3,419\text{ cm}^{-1}$) was covered with the O—H bonds of the $\text{Fe}_{3-x}\text{Ti}_x\text{O}_4$. The observations in Figure 1c showed the peaks for bending vibrations of the N—H bond at 1,555 and 846 cm^{-1} , in addition to the bands of stretching vibration of the NH_3^+ group at $2,736\text{--}3,053\text{ cm}^{-1}$. The bands at $1,662\text{ cm}^{-1}$ (C=O esteric band), $1,488\text{ cm}^{-1}$ (C=C bond), and $1,251\text{ cm}^{-1}$ (C—N bond) confirmed the presence of tryptophan. Finally, Figure 1d contains all the bands of the previous layers in addition to the ethyl iodide part that covered themselves completely made the bands very broad.

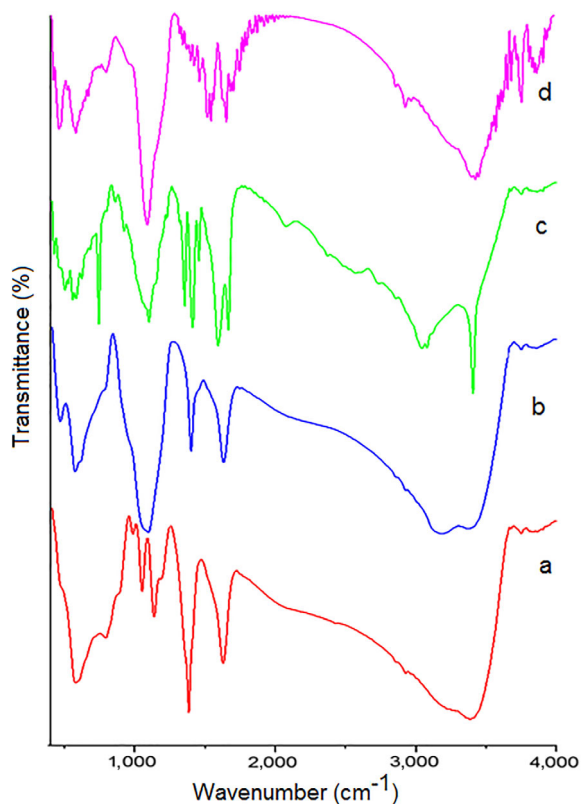


FIGURE 1 The FT-IR spectra of (a) $\text{Fe}_{3-x}\text{Ti}_x\text{O}_4$, (b) $\text{Fe}_{3-x}\text{Ti}_x\text{O}_4\text{-SiO}_2$, (c) $\text{Fe}_{3-x}\text{Ti}_x\text{O}_4\text{-SiO}_2\text{@Trp}$, and (d) nano $\text{Fe}_{3-x}\text{Ti}_x\text{O}_4\text{-SiO}_2\text{@TrpEt}_3^+\text{I}^-$

The thermal stability of the nano $\text{Fe}_{3-x}\text{Ti}_x\text{O}_4\text{-SiO}_2\text{@Trp}$ (Figure 2, top) and the final $\text{Fe}_{3-x}\text{Ti}_x\text{O}_4\text{-SiO}_2\text{@TrpEt}_3^+\text{I}^-$ nanocomposite (Figure 2, down) were investigated by thermogravimetric analysis. The top curve shows initial low mass loss of about 6.2% at 91°C that may be due to outer organic layer decomposition (Trp). Consequential weight loss of about 9.8% at 194°C, 12.89% at 276°C, 14.56% at 379°C, 6.57% at 448°C, and 10.73% at 751°C were also observed. The bottom diagram that related to the final $\text{Fe}_{3-x}\text{Ti}_x\text{O}_4\text{-SiO}_2\text{@TrpEt}_3^+\text{I}^-$ nanostructure deconstructed very low mass loss of about 4.69% at 90°C, which probably related to the release of very slight organic outer part. Then, the nanostructure displays a weight loss of about 1.76% at 165°C, 2.85% at 340°C, 1.21% at 515°C, 0.85% at 590°C, and 1.9% above 800°C. According to the thermal decomposition, the $\text{Fe}_{3-x}\text{Ti}_x\text{O}_4\text{-SiO}_2\text{@TrpEt}_3^+\text{I}^-$ nanohybrid is approximately stable until 800°C with the total weight loss of about 13.26%. The comparison of the thermal behavior of $\text{Fe}_{3-x}\text{Ti}_x\text{O}_4\text{-SiO}_2\text{@Trp}$ (top) and $\text{Fe}_{3-x}\text{Ti}_x\text{O}_4\text{-SiO}_2\text{@TrpEt}_3^+\text{I}^-$ (down) affirmed that embedding ethyl iodide on the inner surface of the $\text{Fe}_{3-x}\text{Ti}_x\text{O}_4\text{-SiO}_2\text{@Trp}$ that causes preparation of $\text{TrpEt}_3^+\text{I}^-$ IL elevates the thermal stability of the whole nanohybrid.

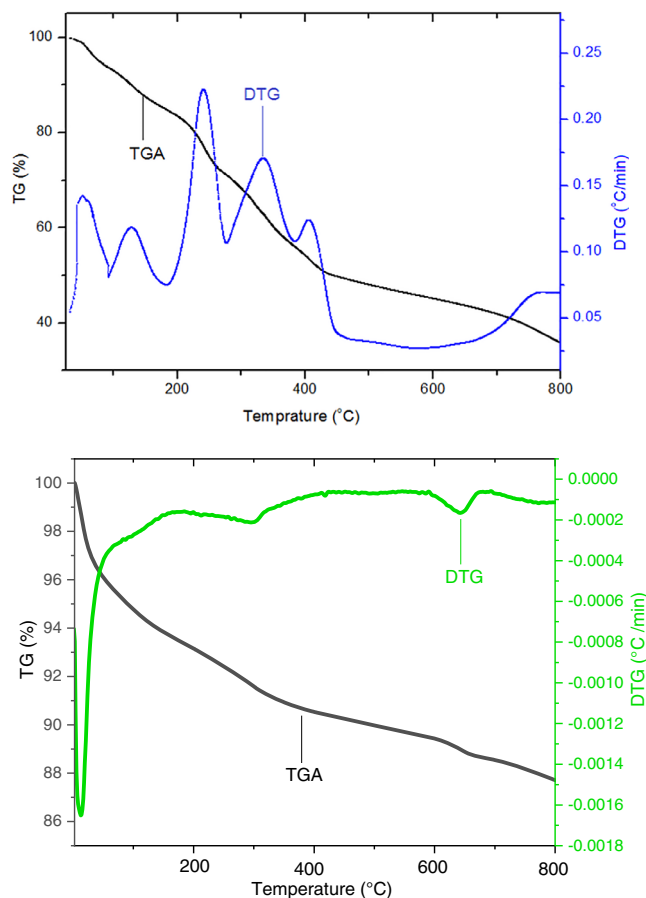


FIGURE 2 TGA/DTG curves of nano $\text{Fe}_{3-x}\text{Ti}_x\text{O}_4\text{-SiO}_2\text{@Trp}$ (top) and nano $\text{Fe}_{3-x}\text{Ti}_x\text{O}_4\text{-SiO}_2\text{@TrpEt}_3^+\text{I}^-$ (bottom)

The field-emission scanning electron microscope (FESEM) image of the synthesized $\text{Fe}_{3-x}\text{Ti}_x\text{O}_4\text{-SiO}_2\text{@TrpEt}_3^+\text{I}^-$ nanocomposite is demonstrated in Figure 3. The average diameter of the nanoparticles is between 10 and 24 nm, with approximately uniform spherical shape.

The results of energy-dispersive X-ray spectroscopy (EDX) of the nano $\text{Fe}_{3-x}\text{Ti}_x\text{O}_4\text{-SiO}_2\text{@TrpEt}_3^+\text{I}^-$ are shown in Figure 4. The data affirmed the presence of Fe (12.68%), Ti (16.20%), Si (13.55%), O (45.36%), C (3.71%), N (2.90%), and I (1.67%) that approved successful synthesis of the nanohybrid. The element Na (1.6%) is due to the sodium hydroxide and sodium nitrate utilized in the synthetic procedure of the nano composite.

The vibrating sample magnetometer (VSM) analysis of the sequential nanocomposite preparation gained in Figure 5 is used to investigate its magnetite behavior. According to the curves a-d, saturation magnetization of 26.091 emu/g for $\text{Fe}_{3-x}\text{Ti}_x\text{O}_4$, 25.905 emu/g for $\text{Fe}_{3-x}\text{Ti}_x\text{O}_4\text{-SiO}_2$, 19.976 emu/g for $\text{Fe}_{3-x}\text{Ti}_x\text{O}_4\text{-SiO}_2\text{@Trp}$, and 18.044 emu/g for $\text{Fe}_{3-x}\text{Ti}_x\text{O}_4\text{-SiO}_2\text{@TrpEt}_3^+\text{I}^-$ confirmed the total superparamagnetism properties. The descending slope in the values related to

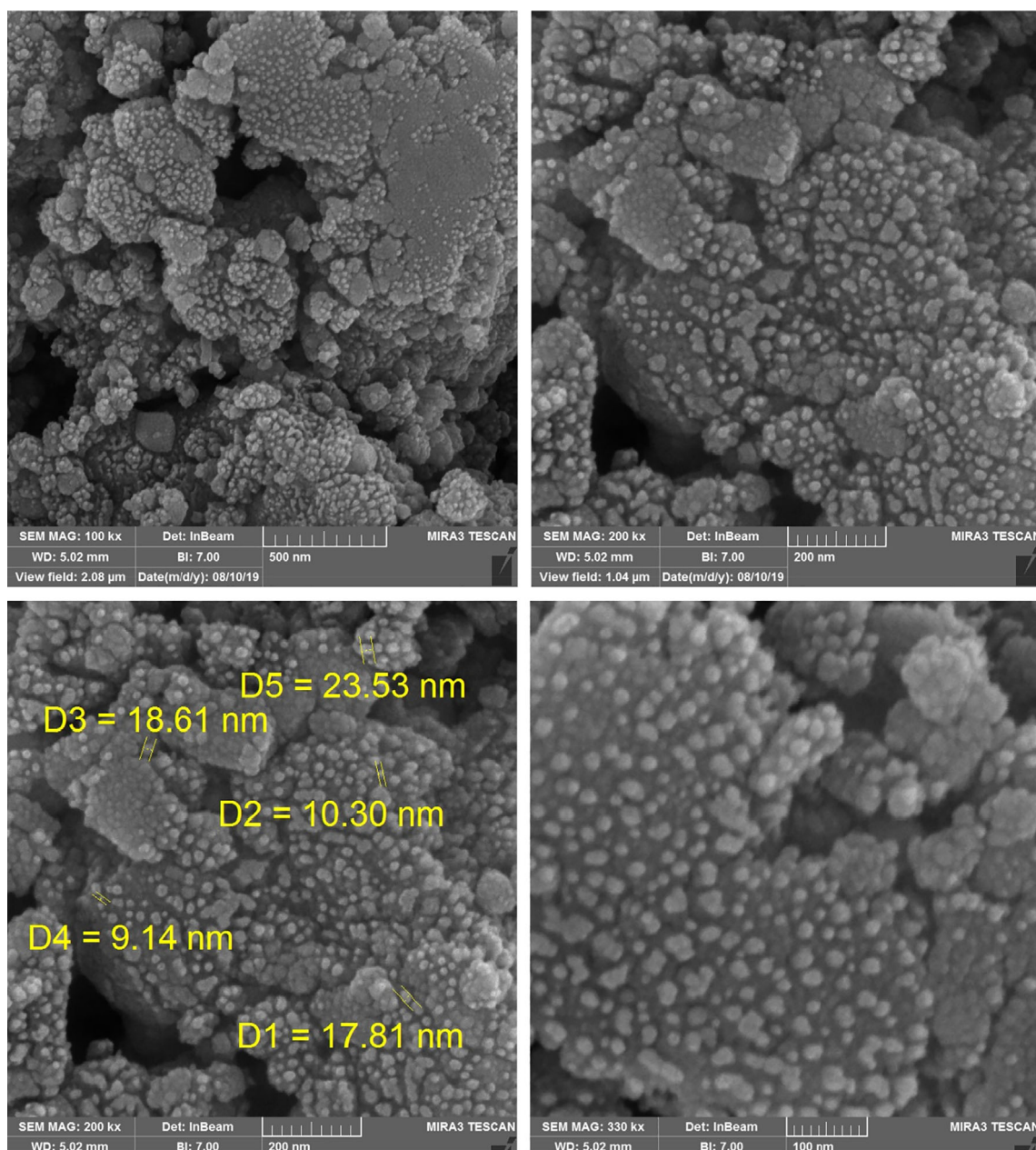


FIGURE 3 FESEM images of $\text{Fe}_{3-x}\text{Ti}_x\text{O}_4\text{-SiO}_2\text{@TrpEt}_3^+\text{I}^-$ nanocomposite

embedding silica, tryptophan, and ethyl iodide on the internal $\text{Fe}_{3-x}\text{Ti}_x\text{O}_4$ core.

X-ray fluorescence (XRF) analysis of the titanomagnetite core and the final $\text{Fe}_{3-x}\text{Ti}_x\text{O}_4\text{-SiO}_2\text{@TrpEt}_3^+\text{I}^-$ nanocomposite are represented in Table 1 (entries 1 and 2, respectively). The Iodine and SiO_2 exhibition along with Fe_2O_3 and TiO_2 affirmed successful preparation of $\text{Fe}_{3-x}\text{Ti}_x\text{O}_4\text{-SiO}_2\text{@TrpEt}_3^+\text{I}^-$ through step-by-step embedding procedure on the initial $\text{Fe}_{3-x}\text{Ti}_x\text{O}_4$ core. In addition, the comparison of the percentages of TiO_2 and Fe_2O_3 in the initial core and final nanocomposite (entries 1 and 2) affirmed the invariable

structure of the $\text{Fe}_{3-x}\text{Ti}_x\text{O}_4$ during the synthesis of the nanocomposite.

2.2 | Investigation of the catalytic activity of $\text{Fe}_{3-x}\text{Ti}_x\text{O}_4\text{-SiO}_2\text{@TrpEt}_3^+\text{I}^-$ in the synthesis of disubstituted quinolone-2-carboxylates library

Initially, to investigate the catalytic efficacy of $\text{Fe}_{3-x}\text{Ti}_x\text{O}_4\text{-SiO}_2\text{@TrpEt}_3^+\text{I}^-$ nanocomposite, the reactions of aniline (**1a**, 1 mmol), DMAD (**2a**, 1 mmol), and phenylacetylene

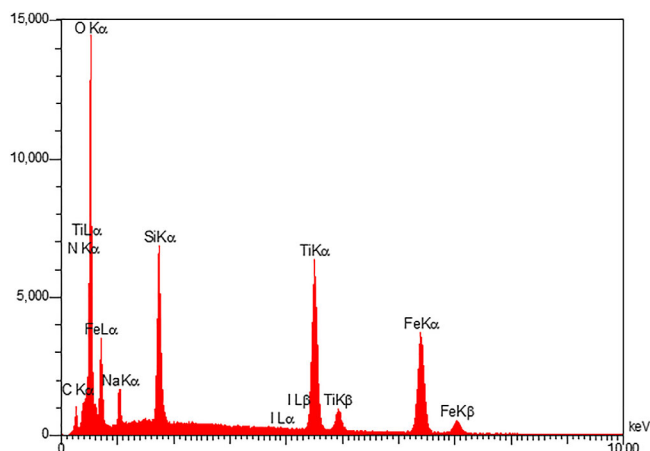


FIGURE 4 EDX analysis of nano $\text{Fe}_{3-x}\text{Ti}_x\text{O}_4\text{-SiO}_2\text{@TrpEt}_3^+\text{I}^-$

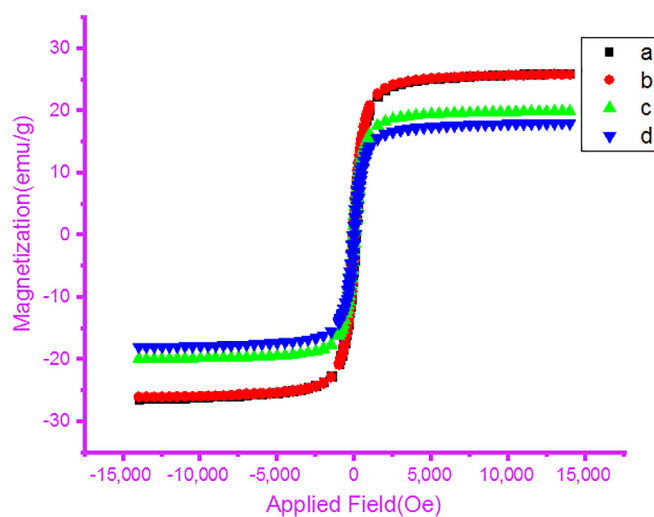


FIGURE 5 VSM magnetization curves of (a) $\text{Fe}_{3-x}\text{Ti}_x\text{O}_4$, (b) $\text{Fe}_{3-x}\text{Ti}_x\text{O}_4\text{-SiO}_2$, (c) $\text{Fe}_{3-x}\text{Ti}_x\text{O}_4\text{-SiO}_2\text{@Trp}$, and (d) $\text{Fe}_{3-x}\text{Ti}_x\text{O}_4\text{-SiO}_2\text{@TrpEt}_3^+\text{I}^-$

TABLE 1 XRF analysis results of the $\text{Fe}_{3-x}\text{Ti}_x\text{O}_4$ core and the final nano $\text{Fe}_{3-x}\text{Ti}_x\text{O}_4\text{-SiO}_2\text{@TrpEt}_3^+\text{I}^-$

	Fe_2O_3	TiO_2	SiO_2	I	LOI	Entry
(%)	46.595	37.462	—	—	11.79	1
(%)	47.779	37.208	8.069	0.055	7.95	2

(**3a**, 1.2 mmol) were applied as the model. According to the results in Table 2, various conditions (catalyst amount, reaction media, and temperature) were examined to obtain the optimized situation. The solvent effect screened by various solvents such as MeOH, EtOH, CH_3CN , and toluene (entries 1–5) and the data affirmed that none of them are appropriate. In the case of entries 3 and 4, no products were observed and the substrates remained intact after the reaction period. In the next

attempt, the model reaction was performed in the absence of solvent at different temperatures (80, 100, and 120°C) and also catalyst amount (entries 6–12). The results demonstrated that doing the reaction at 100°C in the presence of nano $\text{Fe}_{3-x}\text{Ti}_x\text{O}_4\text{-SiO}_2\text{@TrpEt}_3^+\text{I}^-$ (0.12 g) under solvent-free conditions is the best choice (entry 11). The reaction was examined at 120°C but no yield elevation was observed (entry 12). In order to discover more accurate reaction period, the model reaction was repeated in the presence of nano $\text{Fe}_{3-x}\text{Ti}_x\text{O}_4\text{-SiO}_2\text{@TrpEt}_3^+\text{I}^-$ (0.12 g) under solvent-free conditions at 100°C . The results affirmed that the reaction progress occurred up to 18 hr from the beginning and time duration up to 24 does not affect the reaction promotion. In order to recognize the crucial role of nanostructure in the reaction progress, the model reaction was examined in the absence of nano $\text{Fe}_{3-x}\text{Ti}_x\text{O}_4\text{-SiO}_2\text{@TrpEt}_3^+\text{I}^-$ at 100°C within 24 hr. The result demonstrated very low yield (entry 13). In another attempt, the model reaction was examined in the presence of nano $\text{Fe}_{3-x}\text{Ti}_x\text{O}_4\text{-SiO}_2\text{@Trp}$ (0.12 g) at 100°C within 24 hr period. The results showed the reaction progress with 58% yield. The observation affirmed the catalytic role of the IL part in the $\text{Fe}_{3-x}\text{Ti}_x\text{O}_4\text{-SiO}_2\text{@TrpEt}_3^+\text{I}^-$ nanocomposite to elevate the reaction yield. Finally, the optimal conditions were identified in the presence of nano $\text{Fe}_{3-x}\text{Ti}_x\text{O}_4\text{-SiO}_2\text{@TrpEt}_3^+\text{I}^-$ (0.12 g) under solvent-free conditions at 100°C (entry 11).

To spread the efficiency of the route, the reaction of different anilines **1a–g** with dialkyl acetylenedicarboxylates **2a, b**, and terminal alkynes **3a, b** examined under optimized conditions. The results are summarized in Table 3. Various kinds of substituted quinoline-2-carboxylates were obtained via the reaction of anilines and its derivatives with DMAD **2a** and phenylacetylene **3a** successfully (**5a–d**). 1-Butyne **3b**, as an aliphatic acetylenic candidate, performed the reaction very well with aniline/DMAD and 4-hydroxyaniline/DEAD to gain the corresponding quinolines **5e** and **5f**, respectively. Applying 1-naphthylamine in this transformation did not reach satisfactory results and the product methyl 4-phenylbenzo[*h*]quinoline-2-carboxylate **5g** was obtained with 36% yield. Although different aniline derivatives eventuated properly, but in the case of 4-methoxyaniline the yield was few to obtain the product **5h**. Among the eight various quinolines obtained in this scope, two of them are the new compounds (**5e** and **5f**) that are completely characterized by physical and spectral data.

In the next stage, to extend the scope of substituted quinoline-2-carboxylates synthesis, the reaction of anilines **1** with dialkyl acetylenedicarboxylates **2a, b**, and acetophenones **4a–d** was examined (Table 4). The results demonstrated that acetophenone and its derivatives

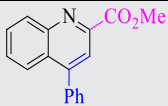
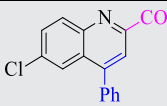
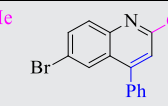
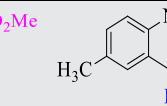
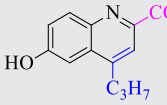
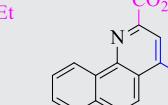
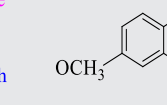
TABLE 2 Screening the reaction conditions to prepare methyl 4-phenylquinoline-2-carboxylate **5a**^a

Entry	Nano Fe _{3-x} Ti _x O ₄ -SiO ₂ @TrpEt ₃ ⁺ I ⁻ (g)	Solvent (5 ml)	Temp (°C)	Yield (%) ^b
1	0.04	MeOH	120	34
2	0.08	MeOH	120	38
3	0.08	EtOH	120	—
4	0.08	CH ₃ CN	120	—
5	0.08	Toluene	100	18
6	0.04	—	80	27
7	0.08	—	100	62
8	0.1	—	80	43
9	0.1	—	100	57
10	0.12	—	80	45
11	0.12	—	100	73
12	0.12	—	120	75
13	—	—	100	10

^aThe substrates **1a**:**2a**:**3a** were used in 1:1:1.2 molar ratio in 24 hr period.

^bIsolated yields.

TABLE 3 Synthesis of substituted quinoline-2-carboxylates **5a–h** from three-component reaction of anilines **1a–g**, dialkyl acetylenedicarboxylates **2a, b**, and terminal alkynes **3a, b**^a

			
5a^c	5b^c	5c^c	5d^c
18 h, 73% ^b	18 h, 65%	20 h, 71%	20 h, 84%
			
5e (new)	5f (new)	5g^c	5h^c
18 h, 75%	15 h, 92%	22 h, 36%	18 h, 12%

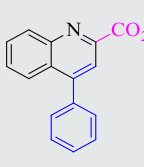
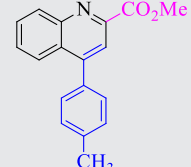
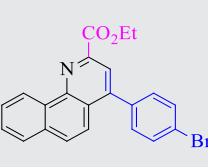
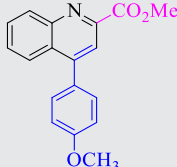
^aReaction conditions: **1** (1 mmol), **2** (1 mmol), **3** (1.2 mmol), nano Fe_{3-x}Ti_xO₄-SiO₂@TrpEt₃⁺I⁻ (0.12 g) at 100°C.

^bIsolated yields.

^cReference of the known compounds is 19.

accomplished the reaction successfully to obtain the correspondence products **5a**, and **5i–l**. In the case of 4-methoxyacetophenone, the reaction progressed in very low yield to obtain the methyl 4-(4-methoxyphenyl)quinoline-2-carboxylate **5l** with 13%. The compounds **5j** and **5k** are the new ones that are characterized completely in the experimental section. It must be mentioned that the reaction examined via A₃-coupling in the presence of benzaldehyde instead of acetophenone in identical conditions within a 24 hr period but no quinoline products were observed.

In continuation to vast quinolines library synthesis, the pseudo three-component reaction of anilines **1** with dialkyl acetylenedicarboxylates **2a, b** was investigated (Table 5). According to the data, aniline and its para-substituted derivatives reacted with DMAD **2a** to obtain the desired 6-substituted quinoline dialkyl-2,4-dicarboxylates **5l–r**. 2-Nitroaniline also achieved the regioselective transformation to afford dimethyl 8-nitroquinoline-2,4-dicarboxylate **5q**. Utilizing DEAD **2b**, as another acetylene ester candidate, generated the corresponding product **5r** in moderate yield.

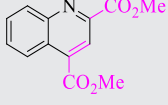
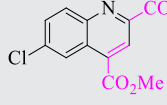
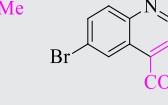
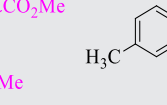
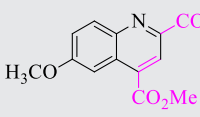
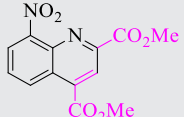
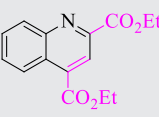
			
5a^c	5i^c	5j (new)	5k^c
19 h, 63% ^b	22 h, 56%	10 h, 77%	20 h, 13%

^aReaction conditions: **1** (1 mmol), **2** (1 mmol), **4** (1.2 mmol), nano Fe_{3-x}Ti_xO₄-SiO₂@TrpEt₃⁺I⁻ (0.12 g) at 100°C.

^bIsolated yields.

^cReference of the known compounds is 16.

TABLE 4 Synthesis of 4-substituted quinoline-2-carboxylates **5** from the reaction of anilines, dialkyl acetylenedicarboxylates **2**, and acetophenones **4^a**

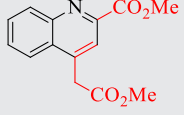
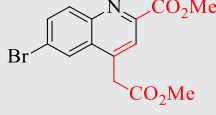
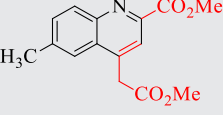
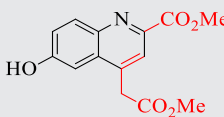
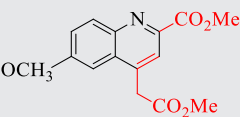
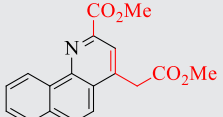
			
5l^c	5m^c	5n^c	5o^c
20 h, 91%	20 h, 84%	20 h, 83%	20 h, 90% ^b
			
5p^c	5q (new)	5r^c	
20 h, 85%	22 h, 82%	21 h, 51%	

^aReaction conditions: **1** (1.0 mmol), **2** (2.2 mmol), and nano Fe_{3-x}Ti_xO₄-SiO₂@TrpEt₃⁺I⁻ (0.12 g) at 100°C.

^bIsolated yields.

^cReference of the known compounds is 16.

TABLE 5 Synthesis of 6-substituted quinoline dialkyl-2,4-dicarboxylates **5l–r** from the reaction of anilines **1**, and dialkyl acetylenedicarboxylates **2^a**

		
5s^c	5t (new)	5u^c
5 h, 91% ^b	7 h, 91%	5 h, 89%
		
5v^c	5w (new)	5x^c
4 h, 95%	5 h, 74%	4 h, 81%

^aReaction conditions: **1** (0.4 mmol), **6** (1.2 mmol), and nano Fe_{3-x}Ti_xO₄-SiO₂@TrpEt₃⁺I⁻ (0.12 g) at 100°C.

^bIsolated yields.

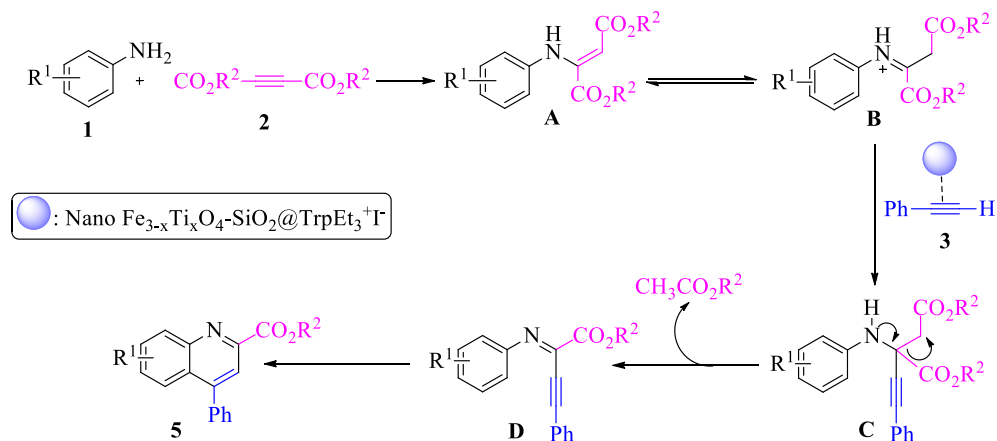
^cReference of the known compounds is 21.

TABLE 6 Synthesis of 6-substituted 4-(2-methoxy-2-oxoethyl)quinoline-2-methylcarboxylates **5t–5y** from the reaction of anilines, and methyl propiolate **6^a**

In order to extend the diversity of the substituted quinoline preparation, the reaction of anilines **1** and methyl propiolate **6** was performed to obtain the desired 6-substituted 4-(2-methoxy-2-oxoethyl)quinoline-

2-methylcarboxylates **5t–5y** (Table 6). Aniline and its para-substituted derivative accomplished the reaction well (**5t–w**). The yield in 4-methoxyaniline usage was moderate in comparison to the other substituents (**5x**).

SCHEME 3 Mechanism for the synthesis of 2,4-disubstituted quinolines



1-Naphthylamine, as a sterically hindered candidate, gave good results to obtain **5y**.

Although the reaction mechanism is not clear completely, a plausible route is proposed in Scheme 3. First, enamine **A** is produced via nucleophilic attack of amine group **1** to dialkyl acetylenedicarboxylates **2**, which isomerized to enamine **B**. The interaction of terminal alkyne **3** with nano $\text{Fe}_{3-x}\text{Ti}_x\text{O}_4\text{-SiO}_2\text{@TrpEt}_3^+\text{I}^-$ formed the activated alkynyl-catalyst species. Subsequent regioselective intermolecular nucleophilic attack of alkynyl-catalyst species to imine **B**, generated intermediate **C**. The propargyl imine **D** was established through a C–C bond cleavage and alkyl acetate removal. Finally, compound **D** underwent intermolecular Friedel–Crafts-type addition leading to annulated final product **5**.^[19] The highlighted feature of this work is the preparation of metal-free activated alkynyl-catalyst species to progress the reaction.

In the next step, the recovery and reusability of the nano $\text{Fe}_{3-x}\text{Ti}_x\text{O}_4\text{-SiO}_2\text{@TrpEt}_3^+\text{I}^-$ were also checked for the synthesis of methyl-4-phenylquinoline-2-carboxylate **5a** through the reaction of aniline (**1a**, 1 mmol), DMAD (**2a**, 1 mmol), and phenylacetylene (**3a**, 1.2 mmol). After completion of the reaction based on the optimized conditions (presence of the 0.12 g of nanohybrid at 100°C within 18 hr period), methanol (10 ml) was added and the nanocatalyst was separated with an external magnet. Washing with further methanol (2 × 5 ml), followed by air-drying for 12 hr, and oven drying at 50°C within 3 hr, the recovered catalyst was used for another cycle to prepare **5a**. The results for three cycles usage demonstrated the high-level catalytic efficacy of the nano $\text{Fe}_{3-x}\text{Ti}_x\text{O}_4\text{-SiO}_2\text{@TrpEt}_3^+\text{I}^-$ to promote the model reaction without significant activity loss (73, 71, and 68% yields, respectively). The FESEM images of the recovered and reused nano $\text{Fe}_{3-x}\text{Ti}_x\text{O}_4\text{-SiO}_2\text{@TrpEt}_3^+\text{I}^-$ are illustrated in Figure 6. The average diameter of nanoparticles is between 20 and 35 nm and the morphology of the nanostructure remained invariable after 3-cycles usage in comparison to the initial nanocomposite.

In the next part, a comparative study of our protocol with previously reported methods is illustrated in Scheme 4. As could be seen, the most highlighted feature of this protocol is performing the reactions in the absence of any additive such as HOTf and $\text{Na}_2\text{S}_2\text{O}_8$. This accomplishment affirms the elevated activity of the nano $\text{Fe}_{3-x}\text{Ti}_x\text{O}_4\text{-SiO}_2\text{@TrpEt}_3^+\text{I}^-$ core-shell. This phenomenon could be according to the synergic effect of each layer utilized in its structure, which leads to its successful operation in the absence of additive. It is also noteworthy that the synthesis of a library of substituted quinolines occurred in the absence of any hazardous solvents such a CH_3CN or MeOH at more reduced temperatures in comparison to the previous methods that made the protocol green and economic.

3 | EXPERIMENTAL

3.1 | General

All chemicals were purchased from the Aldrich, Merck, and Alfa-Aesar companies and used without purification. Melting points were determined by an Electrothermal 9200 apparatus and reported uncorrected. The FT-IR spectra were gained using KBr disks by a Bruker FT-IR (Tensor 27) spectrometer. Magnetization properties were performed by a VSM (MDKB model). Homogenization of the nanostructure was performed in a Wise clean (power of 90 W). ^1H NMR spectra were recorded through a Bruker drx (300 MHz) spectrometer in $\text{DMSO-}d_6$ solvent. The morphology and size of the nanocatalyst were estimated by a FESEM (VEGA \ TESCAN-LMU). Mass spectra were obtained using a Gc-Mass 5973 network mass-selective detector on a Gc 6690 Agilent device. The EDAX was carried out through a TESCAN MIRA III machine. Element percentages were carried out with Philips-PW2404 XRF spectrometer. A centrifuge apparatus (UNIVERSAL 320) operating at 5,000–10,000 rpm was used in the nanocatalyst synthesis procedure.

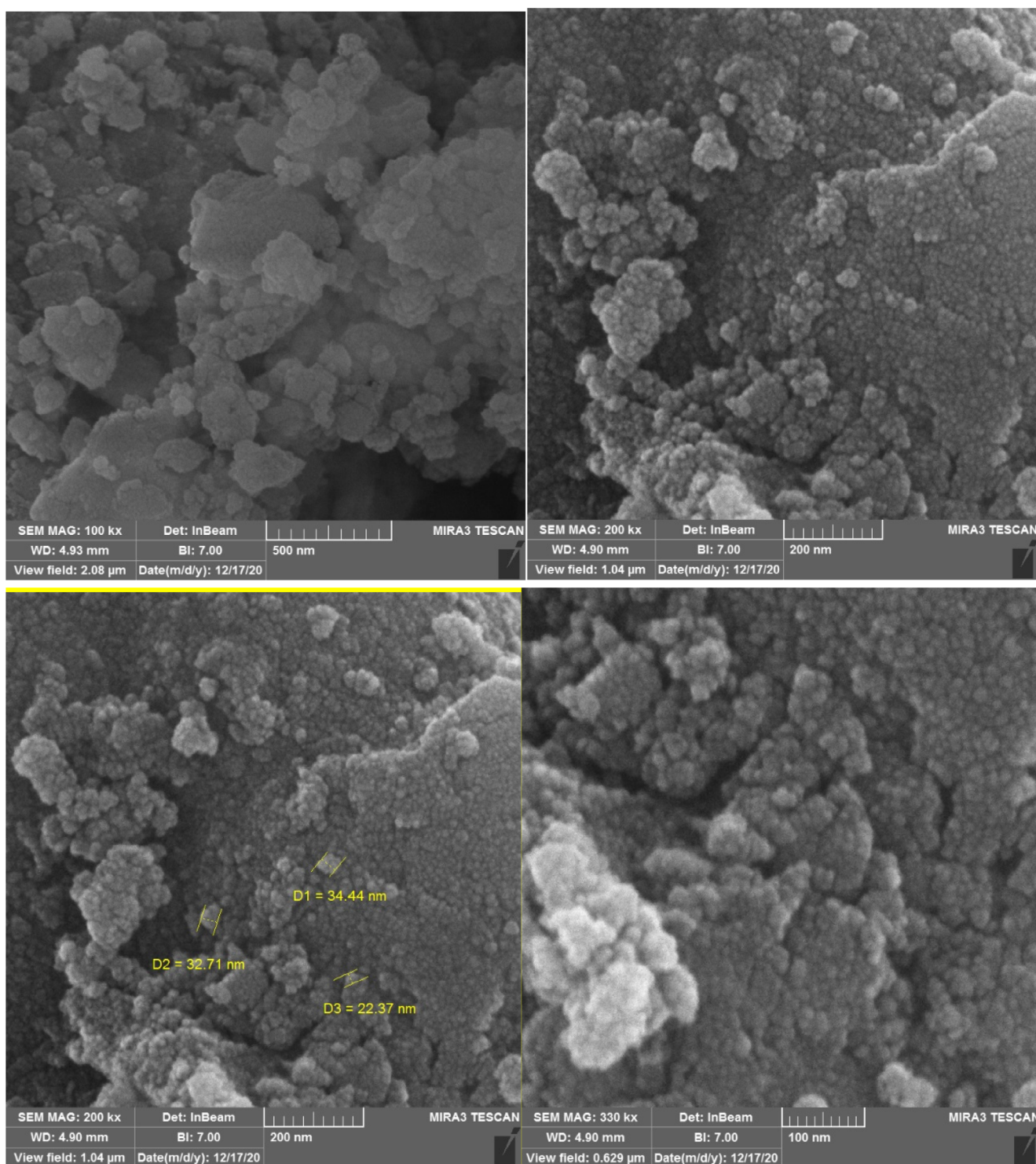


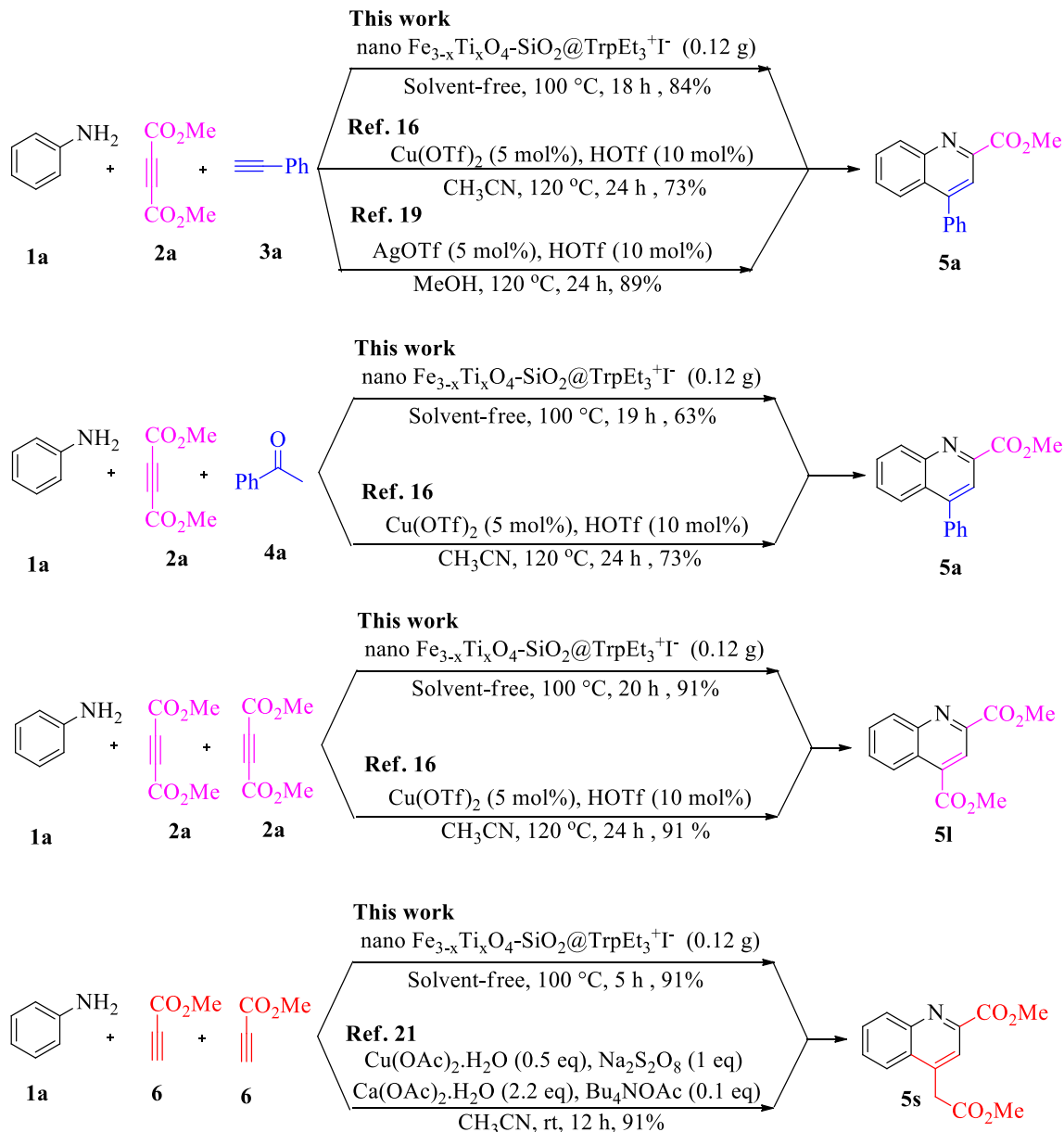
FIGURE 6 FESEM images of the reused nano $\text{Fe}_{3-x}\text{Ti}_x\text{O}_4\text{-SiO}_2\text{@TrpEt}_3^+\text{I}^-$ after three runs

3.2 | Synthetic procedure of nano $\text{Fe}_{3-x}\text{Ti}_x\text{O}_4\text{-SiO}_2\text{@TrpEt}_3^+\text{I}^-$

3.2.1 | Preparation of $\text{Fe}_{3-x}\text{Ti}_x\text{O}_4$

The titanomagnetite ($\text{Fe}_{3-x}\text{Ti}_x\text{O}_4$) was prepared through the previously reported procedure by He group with total

modification.^[32] In a typical modified process, $\text{FeSO}_4 \cdot 7\text{H}_2\text{O}$ (3.81 g) was dispersed in deionized water (18 ml). Then, the aqueous HCl (1 M, 7 ml) was added until reaching pH less than 1. Next, TiCl_4 (1.6 ml) and hydrazine monohydrate (2 ml) were added dropwise to the reaction mixture. The resulting solution was refluxed for 30 min at 90°C under nitrogen atmosphere. In the next step, a



SCHEME 4 Comparison of the work with the previously reported protocols for the synthesis of substituted quinolines

mixture of NaOH (4 g) and NaNO₃ (2 g) in deionized water (18 ml) was added to the reaction mixture and refluxed for 1 hr under vigorous stirring. Finally, the mixture was cooled in room temperature and the solid separated through an external magnet, followed by washing with water (3 × 10 ml) and air-drying to obtain the Fe_{3-x}Ti_xO₄ as black powder.

3.2.2 | Preparation of Fe_{3-x}Ti_xO₄-SiO₂

In a flask, nano Fe_{3-x}Ti_xO₄ powder (1 g) was dispersed in a mixture of ammonia (25 wt%, 2 ml), deionized water (20 ml), and ethanol (60 ml) and sonicated in a bath for 30 min. Next, a mixture of TEOS (0.5 ml) in ethanol (1 ml)

was added dropwise into the Fe_{3-x}Ti_xO₄ solution under vigorous stirring at room temperature, followed by stirring for 20 hr at room temperature. Finally, the product was separated by an external magnet, washed with absolute ethanol (3 × 5 ml), and dried at 70 °C for 5 hr to get Fe_{3-x}Ti_xO₄-SiO₂.

3.2.3 | In situ assembling of the triethyltryptanium iodide IL (TrpEt₃⁺I⁻) on silicated titanomagnetite core to prepare nano Fe_{3-x}Ti_xO₄-SiO₂@TrpEt₃⁺I⁻

A mixture of Fe_{3-x}Ti_xO₄-SiO₂ (1 g) and tryptophan (0.75 g) in diethyl ether (10 ml) was stirred at room

temperature for 2 hr. Next, chloroform (10 ml) was added and the solid was separated by centrifugation (15 min), followed by washing with further chloroform (2×10 ml). The black powder ($\text{Fe}_{3-x}\text{Ti}_x\text{O}_4\text{-SiO}_2\text{@Trp}$) was air-dried for 2 hr at room temperature and oven-dried at 50°C for 1 hr. Next, a mixture of the obtained powder (1 g) and ethyl iodide (2 g) in 20 ml water/ethanol (1:1) was refluxed at 90°C within 3 hr. The residue was separated through centrifuging and washing by equimolar water/ethanol solution (3×10 ml). The final nano $\text{Fe}_{3-x}\text{Ti}_x\text{O}_4\text{-SiO}_2\text{@TrpEt}_3^+\text{I}^-$ was obtained by heating at 50°C for 2 hr (Scheme 1).

3.3 | Synthetic procedure of triethyltryptophanium iodide IL ($\text{TrpEt}_3^+\text{I}^-$)

A mixture of tryptophan (1 g) in ethyl iodide (2.5 g) in deionized water (10 ml) and ethanol (10 ml) was refluxed at 90°C for 18 hr. The residue was separated through centrifuging and washing by equimolar water/ethanol solution (3×10 ml). The final $\text{TrpEt}_3^+\text{I}^-$ IL obtained by heating at 50°C for 2 hr as bright white crystals. Mp = 270°C . IR (KBr, cm^{-1}): 3,404, 3,077, 3,035, 2,852, 2,730, 2,561, 1,666, 1,483, 1,455, 1,414, 1,354, 1,249, 1,208, 1,007, 966, 920, 803, 862, 527, 505, 424. ^1H NMR (300 MHz, $\text{DMSO-}d_6$): 1.04 (m, 6H, 3CH_2), 3.22–3.75 (m, 9H, 3CH_3), 4.01 (s, 2H, CH_2), 9.98–7.04 (m, 2H, Ar), 7.36–7.50 (m, 3H, Ar), 7.60 (brs, 1H, NH), 11.05 ((brs, 1H, OH). MS (ESI) m/z 416 $[\text{M}^+]$, 401 ($[\text{M}^+]-\text{Me}$), 358 ($[\text{M}^+]-\text{Me}, -\text{CO}_2\text{H}$), 329 ($[\text{M}^+]-3\text{Et}$), 284 ($[\text{M}^+]-3\text{Et}, -\text{CO}_2\text{H}$), 202 ($[\text{M}^+]-3\text{Et}, -\text{I}$), 188 ($[\text{M}^+]-\text{NEt}_3, -\text{I}$), 171 ($[\text{M}^+]-\text{C}_3\text{H}_7\text{I}$), 156 (EtI), 143 ($[\text{M}^+]-\text{NEt}_3, -\text{CO}_2\text{H}, -\text{I}$), 130 (3-methylindolyl), 44(CO_2).

3.4 | General procedure for the synthesis of 4,6-disubstituted quinolone-2-carboxylates (5a–l)

A mixture of anilines (**1a–g**, 1 mmol), dialkyl acetylenedicarboxylates (**2a, b**, 1 mmol), and terminal alkynes **3a, b** or acetophenones **4a–d** (1.2 mmol) in the presence of nano $\text{Fe}_{3-x}\text{Ti}_x\text{O}_4\text{-SiO}_2\text{@TrpEt}_3^+\text{I}^-$ (0.12 g) were stirred at 100°C in air. The progress of the reaction was investigated by TLC (*n*-hexane/EtOAc eluent, 2:1). After completion, methanol (10 ml) was added to the mixture and the nanocatalyst was separated by an external magnet. Purification was accomplished through plate chromatography on silica gel to afford the desired products **5a–k** (Scheme 1a, Tables 3 and 4).

3.4.1 | Methyl 4-propylquinoline-2-carboxylate (5e)

Orange solid. Mp: $95\text{--}98^\circ\text{C}$. IR (KBr, cm^{-1}): 3,004, 2,955, 2,922, 2,852, 1,740, 1,646, 1,437. ^1H NMR (300 MHz, $\text{DMSO-}d_6$): 1.22–1.32 (m, 3H, CH_3), 3.40–3.47 (m, 2H, CH_2), 3.57–3.62 (m, 2H, CH_2), 3.7 (s, 3H, CH_3), 6.90–6.95 (m, 1H, Ar), 7.03–7.07 (m, 1H, Ar), 7.14–7.29 (m, 2H, Ar), 7.75 (d, $J = 8.19$ Hz, 1H, Ar). ^{13}C NMR (75 MHz, $\text{DMSO-}d_6$): 52.27, 52.70, 119.87, 120.49, 128.54, 129.27, 129.45, 161.79, 166.66. MS (ESI) m/z 229 $[\text{M}^+]$, 214 ($[\text{M}^+]-\text{Me}$), 198 ($[\text{M}^+]-\text{OMe}$), 183 ($[\text{M}^+]-\text{OMe}, -\text{Me}$), 169 ($[\text{M}^+]-\text{OMe}, -\text{Et}$), 155 ($[\text{M}^+]-\text{OMe}, -\text{C}_3\text{H}_7$), 59 (CO_2Me), 43 (C_3H_7).

3.4.2 | Ethyl 6-hydroxy-4-propylquinoline-2-carboxylate (5f)

Orange solid. Mp: $81\text{--}83^\circ\text{C}$. IR (KBr, cm^{-1}): 3,443, 2,923, 2,853, 1,740, 1,663, 1,463, 1,020. ^1H NMR (300 MHz, $\text{DMSO-}d_6$): 0.88 (t, $J = 7.05$ Hz, 3H, CH_3), .1.7 (t, $J = 7.1$ Hz, 3H, CH_3), 1.21–1.29 (m, 2H, CH_2), 3.84–3.92 (m, 2H, CH_2), 4.14 (q, $J = 7.14$ Hz, 2H, CH_2), 4.39 (bs, 1H, OH), 6.61–6.68 (m, 1H, Ar), 6.70–6.77 (m, 2H, Ar), 6.82 (d, $J = 8.6$ Hz, 1H, Ar). ^{13}C NMR (75 MHz, $\text{DMSO-}d_6$): 13.16, 13.85, 60.29, 61.82, 105.14, 114.91, 120.31–122.09, 128.81, 142.93, 146.02, 154.49, 158.35, 164.94. MS (ESI) m/z 259 $[\text{M}^+]$, 242 ($[\text{M}^+]-\text{OH}$), 226 ($[\text{M}^+]-\text{OH}, -\text{Me}$), 216 ($[\text{M}^+]-\text{C}_3\text{H}_7$), 214 ($[\text{M}^+]-\text{OEt}$), 198 ($[\text{M}^+]-\text{OH}, -\text{C}_3\text{H}_7$), 170 ($[\text{M}^+]-\text{OEt}, -\text{C}_3\text{H}_7$), 152 ($[\text{M}^+]-\text{OEt}, -\text{C}_3\text{H}_7, -\text{OH}$), 125 (6-quinolinol).

3.5 | General procedures for the synthesis of 6-substituted quinoline dialkyl-2,4-dicarboxylates (5l–5r)

A mixture of anilines (**1**, 1 mmol) and dialkyl acetylenedicarboxylates (**2**, 2.2 mmol) in the presence of nano $\text{Fe}_{3-x}\text{Ti}_x\text{O}_4\text{-SiO}_2\text{@TrpEt}_3^+\text{I}^-$ (0.12 g) were stirred at 100°C until appropriate time monitored by TLC (*n*-hexane/EtOAc eluent, 2:1). Next, methanol (10 ml) was added and the catalyst was separated with an external magnet. Purification of the products was done through PLC to obtain the products **5l–5r** (Scheme 1b and Table 5).

3.5.1 | Ethyl 4-(4-bromophenyl)benzo[h]quinoline-2-carboxylate (5j)

Brown solid. Mp: 84°C . IR (KBr, cm^{-1}): 2,982, 2,971, 2,855, 1,726, 1,632, 1,466, 1,114, 1,040, 832. ^1H NMR

(300 MHz, DMSO- d_6): 1.06–1.22 (m, 2H, CH₂), 4.08–4.31 (m, 3H, CH₃), 7.39–7.42 (m, 1H, Ar), 7.44–7.57 (m, 4H, Ar), 7.69–7.72 (m, 1H, Ar), 7.96 (d, $J = 7.56$ Hz, 2H, Ar), 8.06 (d, $J = 7.98$ Hz, 2H, Ar). ¹³C NMR (75 MHz, DMSO- d_6): 14.82, 61.17, 121.19, 122.55, 124.60, 125.48, 125.73, 126.45, 126.62, 127.03, 128.35, 133.84, 136.29, 143.69, 147.49, 159.14, 165.30. MS (ESI) m/z 407 [M⁺], 326 ([M⁺]-Br), 311 ([M⁺]-Br, -Me), 282 ([M⁺]-Br, -OEt), 255 ([M⁺]-Br, -CO₂Et), 205 ([M⁺]-BrPh, -OEt), 168 (bromotolyl), 127(naphthyl).

3.5.2 | Dimethyl 8-nitroquinoline-2,4-dicarboxylate (5q)

Orange solid. Mp: 92–96°C. IR (KBr, cm⁻¹): 3,005, 2,956, 2,924, 2,852, 1,870, 1,736, 1,638, 1,524, 1,437, 135, 1,170, 1,020. ¹H NMR (300 MHz, DMSO- d_6): 3.53 (s, 3H, CH₃), 3.68 (s, 3H, CH₃), 6.81 (d, $J = 8.55$ Hz, 1H, Ar), 7.05–7.14 (m, 1H, Ar), 7.65–7.66 (m, 1H, Ar), 8.15 (d, $J = 7.92$ Hz, 1H, Ar). MS (ESI) m/z 290 [M⁺], 275 ([M⁺]-Me), 244 ([M⁺]-Me, -OMe), 228 ([M⁺]-2OMe), 198 ([M⁺]-OMe, -Me, -NO₂), 184 ([M⁺]-2OMe, -NO₂), 156 ([M⁺]-OMe, -CO₂Me, -NO₂), 135 (nitroaniline), 128 ([M⁺]-2CO₂Me, -NO₂), 91 (aniline), 59 (CO₂Me), 44 (NO₂).

3.6 | General procedures for the synthesis of 6-substituted 4-(2-methoxy-2-oxoethyl)quinoline-2-methylcarboxylates (5s–5x)

A mixture of anilines (**1**, 0.4 mmol), methyl propiolate (**6**, 1.2 mmol), and nano Fe_{3-x}Ti_xO₄-SiO₂@TrpEt₃⁺I⁻ (0.12 g) were stirred at 100°C until completion and investigated by TLC (*n*-hexane/EtOAc eluent, 2:1). Next, methanol (10 ml) was added and the catalyst was separated with an external magnet. Purification of the products was done through PLC to obtain the products **5s–5x** (Scheme 1c and Table 6).

3.6.1 | Methyl 6-bromo-4-(2-methoxy-2-oxoethyl)quinoline-2-carboxylate (5t)

Yellow solid. Mp: 72–75°C. IR (KBr, cm⁻¹): 3,098, 3,003, 2,924, 2,853, 1,732, 1,667, 1,609, 1,441, 1,201, 842. ¹H NMR (300 MHz, DMSO- d_6): 3.61–3.62 (s, 3H, CH₃), 3.66–3.97 (s, 2H, CH₂), 3.77 (s, 3H, OCH₃), 7.23–7.25 (m, 1H, Ar), 7.41–7.46 (m, 1H, Ar), 7.52–7.56 (m, 1H, Ar), 8.61 (s, 1H, Ar). ¹³C NMR (75 MHz, DMSO- d_6): 38.66, 50.29, 51.24, 52.77, 130.94, 132.20, 133.42, 135.80, 138.94, 142.87–143.00, 149.11, 164.54, 167.71.

MS (ESI) m/z 338 [M⁺], 257 ([M⁺]-Br), 227 ([M⁺]-Br, -OMe), 197 ([M⁺]-Br, -CO₂Me), 184 ([M⁺]-Br, -CH₂CO₂Me), 171 (bromoaniline), 156 (bromophenyl), 89 (CH₃CH₂CO₂Me), 76 (Ph), 73 (CH₃CO₂Me), 59 (CO₂Me).

3.6.2 | Methyl 6-methoxy-4-(2-methoxy-2-oxoethyl)quinoline-2-carboxylate (5w)

Yellow solid. Mp: 55°C. IR (KBr, cm⁻¹): 3,029, 3,002, 2,952, 2,923, 2,851, 1,735, 1,621, 1,512, 1,435, 823. ¹H NMR (300 MHz, DMSO- d_6): 3.54–3.55 (m, 2H, CH₂), 3.62 (s, 3H, OCH₃), 3.65 (s, 3H, OCH₃), 3.7 (s, 3H, OCH₃), 6.43 (d, $J = 8.83$ Hz, 1H, Ar), 6.77 (s, 1H, Ar), 6.95 (d, $J = 8.9$ Hz, 1H, Ar), 7.65 (s, 1H, Ar). MS (ESI) m/z 289 [M⁺], 274 ([M⁺]-Me), 258 ([M⁺]-OMe), 243 ([M⁺]-Me, -OMe), 227 ([M⁺]-2OMe), 199 ([M⁺]-CO₂Me, -OMe), 168 ([M⁺]-CO₂Me, -2OMe), 137 (2-methyl-4-methoxyaniline), 122 (4-methoxyaniline), 77 (Ph).

4 | CONCLUSIONS

In this research, a novel nanostructure was prepared from the titanomagnetite that was covered with silica, tryptophan amino acid, and ethyl iodide consequently (Fe_{3-x}Ti_xO₄-SiO₂@TrpEt₃⁺I⁻). The tryptophan and ethyl iodide were converted to the triethyltryptophanium iodide IL in situ. The obtained nano inorganic-bio-organic core-shell was characterized by FESEM, EDAX, FT-IR, TGA/DTG, VSM, and XRF techniques. Its catalytic efficacy was examined to yield a vast library of substituted quinolone-2-carboxylates from different annulation MCRs such as three-component reaction of aromatic amines, dialkyl acetylenedicarboxylates, and terminal alkenes/ketones; pseudo three-component reaction of anilines and dialkyl acetylenedicarboxylates; and pseudo three-component reaction of anilines and methyl propiolate under solvent-free conditions at 100°C. The notable points of this procedure are regioselective preparation of a wide-spread class of substituted quinolines, green reaction media in the absence of any solvents, and hazardous additives, and simple work-up procedure due to separation from the nanocatalyst via an external magnet. The protocol exhibited new mild outlook to obtain substituted quinolines.

ACKNOWLEDGMENT

The authors thank to Alzahra University Research Council for support of this work.

ORCID

Kobra Nikoofar  <https://orcid.org/0000-0002-3950-8229>

REFERENCES

- [1] S. Li, L. Hu, J. Li, J. Zhu, F. Zeng, Q. Huang, L. Qiu, R. Du, R. Cao, *Eur. J. Med. Chem.* **2019**, *162*, 666.
- [2] K. D. Upadhyay, N. M. Dodia, R. C. Khunt, R. S. Chaniara, A. K. Shah, *ACS Med. Chem. Lett.* **2018**, *9*, 283.
- [3] C. De la Guardia, D. E. Stephens, H. T. Dang, M. Quijada, O. V. Larionov, R. Leonart, *Molecules* **2018**, *23*, 672.
- [4] K. Kaur, M. Jain, R. P. Reddy, R. Jain, *Eur. J. Med. Chem.* **2010**, *45*, 3245.
- [5] Y. Fang, R. Zhang, Z. Shen, H. Wu, C. Tan, J. Weng, T. Xu, X. Liu, *J. Heterocycl. Chem.* **2018**, *55*, 240.
- [6] R. Watpade, A. Bholay, R. Toche, *J. Heterocycl. Chem.* **2017**, *54*, 3434.
- [7] W. Gu, X. Jin, D. Li, S. Wang, X. Bing, T. H. Chen, *Inorg. Med. Chem. Lett.* **2017**, *27*, 4128.
- [8] M. M. R. Moran, J. E. Angel Guio, N. H. Cano, B. Migliore, R. Izquierdo, J. Charris, S. Lopez, A. Israel, A. Santiago, R. Rossi, L. Perdomo, A. S. Dabian, M. V. Sosa, A. Villalba, L. B. A. Migliore, *Letts. Drug Des. Discov.* **2018**, *15*, 294.
- [9] N. Chokkar, S. Kalra, M. Chauhan, R. Kumar, *Mini-Rev. Med. Chem.* **2019**, *19*, 510.
- [10] T. G. Shruthi, S. Eswaran, P. Shivarudraiah, S. Narayanan, S. Subramanian, *Bioorg. Med. Chem. Lett.* **2019**, *29*, 97.
- [11] J. P. S. Ferreira, S. M. Cardoso, F. A. Almeida Paz, A. M. S. Silva, V. L. M. Silva, *New J. Chem.* **2020**, *44*, 6501.
- [12] A. Minić, T. de Walle, K. Hecke, J. Combrinck, P. J. Smith, K. Chibale, M. D'hooghe, *Eur. J. Med. Chem.* **2002**, *187*, 111963.
- [13] D. Maity, A. Mukherjee, S. Kumar, M. Partha Roy, *J. Lumin.* **2019**, *210*, 508.
- [14] V. V. Menon, E. Fazal, Y. S. Mary, C. Y. Panicker, S. Armaković, S. J. Armaković, S. Nagarajan, C. V. Alsenoy, *J. Mol. Struct.* **2017**, *1127*, 124.
- [15] P. Tangudom, E. Wimolmala, B. Prapagdee, N. Sombatsompop, *Polym. Test.* **2019**, *79*, 106023.
- [16] W. Wu, Y. Guo, X. Xu, Z. Zhou, X. Zhang, B. Wu, W. Yi, *Org. Chem. Front.* **2018**, *5*, 1713.
- [17] M. Zhong, S. Sun, J. Cheng, Y. Shao, *J. Org. Chem.* **2016**, *81*, 10825.
- [18] S. Naidoo, V. Jeena, *Synthesis* **2017**, *49*, 2621.
- [19] Y. Li, Q. Zhang, X. Xu, X. Zhang, Y. Yang, W. Yi, *Tetrahedron Lett.* **2019**, *60*, 965.
- [20] D. S. Bose, N. Ramesh, *Synth. Commun.* **2020**, *50*, 1495.
- [21] H. Dai, C. Li, C. Yu, Z. Wang, H. Yan, C. Lu, *Org. Chem. Front.* **2017**, *4*, 2008.
- [22] A. S. G. Prasad, A. GopiReddy, V. N. B. Tokala, K. Deepthi, T. B. Rao, M. V. B. Rao, *Chem. Data Collect.* **2020**, *28*, 100469.
- [23] Z. A. Nima, F. Watanabe, A. Jamshidi-Parsian, M. Sarimollaoglu, D. A. Nedosekin, M. Han, J. A. Watts, A. S. Biris, V. P. Zharov, E. I. Galanzha, *Sci. Rep.* **2019**, *9*, 887.
- [24] M. Ferreira, J. Sousa, A. Pais, C. Vitorino, *Material.* **2020**, *13*, 266.
- [25] G. R. Rodrigues, C. López-Abarrategui, I. S. Gómez, S. C. Dias, A. J. Otero-González, O. L. Franco, *Int. J. Pharm.* **2019**, *555*, 356.
- [26] M. Hasanzadeh, A. Karimzadeh, N. Shadjou, A. Mokhtarzadeh, L. Bageri, S. Sadeghi, S. Mahboob, *Mat. Sci. Engin. C* **2016**, *68*, 814.
- [27] H. Fatima, K. Kim, *Adv. Powder Technol.* **2018**, *29*, 2678.
- [28] A. Masudi, G. E. Harimisa, N. Abdul Ghafar, N. W. Che Jusoh, *Environ. Sci. Pollut. Res.* **2020**, *27*, 4664.
- [29] L. Hou, L. Wang, S. Royer, H. Zhang, *J. Hazard. Mater.* **2016**, *302*, 458.
- [30] A. R. Brown, A. Hart, V. S. Coker, J. R. Lloyd, J. Wood, *Fuel* **2016**, *185*, 442.
- [31] A. Baeza, G. Guillena, D. J. Ramón, *Chemcatchem* **2016**, *8*, 49.
- [32] S. Yang, H. He, D. Wu, D. Chen, X. Liang, Z. Qin, M. Fan, J. Zhu, P. Yuan, *Appl. Catal. B-Environ.* **2009**, *89*, 527.
- [33] D. Azarifar, O. Badalkhani, Y. Abbasi, M. Hasanabadi, *J. Iran. Chem. Soc.* **2017**, *14*, 403.
- [34] D. Azarifar, Y. Abbasi, *Synth. Commun.* **2016**, *46*, 745.
- [35] D. Azarifar, Y. Abbasi, O. Badalkhani, *Appl. Organometal. Chem.* **2018**, *32*, e3939.
- [36] D. Azarifar, Y. Abbasi, M. Jaymand, M. A. Zolfigol, M. Ghaemi, O. Badalkhani, *J. Organomet. Chem.* **2019**, *895*, 55.
- [37] D. Azarifar, O. Badalkhani, M. Chehregosha, M. Jaymand, *Chem. Chem. Technol.* **2020**, *14*, 62.
- [38] R. L. Vekariya, *J. Mol. Liq.* **2017**, *227*, 44.
- [39] B. Karimi, M. Tavakolian, M. Akbari, F. Mansouri, *ChemistrySelcet* **2018**, *10*, 3173.
- [40] B. Xin, C. Jia, X. Li, *Curr. Org. Chem.* **2016**, *20*, 616.
- [41] S. Zhang, L. Ma, P. Wen, X. Ye, R. Dong, W. Sun, M. Fan, D. Yang, F. Zhou, W. Liu, *Tribol. Int.* **2018**, *121*, 435.
- [42] W. Chen, Y. Zhang, L. Zhu, J. Lan, R. Xie, J. You, *J. Am. Chem. Soc.* **2007**, *129*, 13879.
- [43] Q. Liu, K. Wu, F. Tang, L. Yao, F. Yang, Z. Nie, S. Yao, *Chem. Eur. J.* **2009**, *15*, 9889.
- [44] Q. Yang, Z. Wang, Z. Bao, Z. Zhang, Y. Yang, Q. Ren, H. Xing, S. Dai, *ChemSusChem.* **2016**, *9*, 806.
- [45] S. Fujiwara, H. Ohno, M. Yoshio, T. Kato, T. Ichikawa, *Bull. Chem. Soc. Jpn.* **2018**, *91*, 1.
- [46] M. P. Pereira, R. Martins, M. A. L. de Oliveira, F. I. Bombonato, *RSC Adv.* **2018**, *8*, 23903.
- [47] P. Ossowicz, Z. Rozwadowski, M. Gano, E. Janus, *Pol. J. Chem. Technol.* **2016**, *18*, 90.
- [48] R. Figueroa Guñez, J. G. Santos, R. A. Tapia, J. J. Alcazar, M. E. Aliaga, P. Pavez, *Pure Appl. Chem.* **2020**, *92*, 97.
- [49] F. Yu, Y. Chi, C. H. Gao, R. Chen, C. Xie, Sh. Yu, *Chem. Res. Chin. Univ.* **2020**, *36*, 865. <https://doi.org/10.1007/s40242-019-9186-z>.
- [50] K. Nikoofar, F. Shahriyari, *Polyhedron* **2020**, *179*, 114361.
- [51] K. Nikoofar, S. S. Peyrovehbaghi, *J. Chin. Chem. Soc.* **2020**, *67*, 1303.
- [52] K. Nikoofar, F. Molaie Yielzoleh, *Res. Chem. Intermed.* **2018**, *44*, 7353.
- [53] K. Nikoofar, H. Heidari, Y. Shahedi, *Cellulose* **2018**, *25*, 5697.
- [54] K. Nikoofar, S. Khani, *Catal. Lett.* **2018**, *148*, 1651.

How to cite this article: Nikoofar K, Molaie Yielzoleh F. Cascade embedding triethyltryptophanium iodide ionic liquid (TrpEt₃⁺I⁻) on silicated titanomagnetite core (Fe_{3-x}Ti_xO₄-SiO₂@TrpEt₃⁺I⁻): A novel nano organic-inorganic hybrid to prepare a library of 4-substituted quinoline-2-carboxylates and 4,6-disubstituted quinoline-2-carboxylates. *J Chin Chem Soc.* 2021;1-14. <https://doi.org/10.1002/jccs.202000444>